

Study of Human Calcitonin Fibrillation by Proton Nuclear Magnetic Resonance Spectroscopy

Kenji Kanaori and Atsuko Y. Nosaka*

International Research Laboratories, Ciba-Geigy Japan Ltd., P.O. BOX 1, Takarazuka 665, Japan

*Received May 23, 1995**

ABSTRACT: The fibrillation of human calcitonin (hCT) has been investigated by NMR in aqueous solution. The time course of proton one- and two-dimensional NMR spectra of hCT (80 mg/mL at pH 2.9) was measured during the fibrillation. It showed a gradual broadening of the peptide peaks, followed by a rapid broadening and subsequent disappearance of the peaks. The gradual broadening can be attributed to equilibrium between monomer and associated hCT, whereas the rapid broadening can be attributed to formation of aggregates and to gelation of the peptide solution. All the peptide peaks did not broaden and disappear simultaneously. Peaks of residues in the N-terminal (Cys¹–Cys⁷) and central (Met⁸–Pro²³) regions broadened and disappeared faster during the gradual broadening than those in the C-terminal region (Gln²⁴–Pro³²). Moreover, in the N-terminal and central residues, peaks of Cys¹, Leu^{4,9}, Met⁸, Tyr¹², Asp¹⁵, and Phe^{16,19,22} disappeared faster than those of Asn^{3,17}, Ser⁵, Cys⁷, Gln¹⁴, Lys¹⁸, and His²⁰. Hydrogen–deuterium exchange of amide protons indicated the formation of hydrogen bonds caused by association of hCT molecules. The amphiphilicity of the peptide appears to be important for the hCT association.

Calcitonin (CT)¹ is a single polypeptide hormone which consists of 32 amino acids with an N-terminal disulfide bridge between positions 1 and 7 and a C-terminal proline amide residue. CT plays an important role in calcium–phosphorus metabolism (Copp et al., 1962; Kumar et al., 1963; Austin & Heath, 1981) and is used as treatment for various diseases, notably osteoporosis. However, human CT (hCT) easily associates and precipitates as insoluble fibrils upon storing in aqueous solution, which is a defect in therapeutic use. The understanding of the fibrillation process and of the hCT folding mechanism is expected to contribute to the further improvement of the long time stable aqueous therapeutic formulations of hCT (Arvinte & Ryman, 1992).

Early studies of the hCT association by electron microscopy revealed that it consists of fibrils of 80 Å in diameter, which often associate with one another (Sieber et al., 1970). Recently, Arvinte et al. (1993) studied the kinetics of hCT fibrillation by turbidity and electron microscopy measurements and demonstrated that the fibrillation mechanism conforms to the double nucleation mechanism (Ferrone et al., 1980, 1985; Samuel et al., 1990).

The hCT fibrillation was also investigated by circular dichroism (CD), fluorescence, and Fourier transform infrared spectroscopy (FTIR) (Arvinte et al., 1993). These spectroscopic studies showed that hCT molecules form α -helical and intermolecular β -sheet secondary structure components,

approximately 24 h after dissolving the peptide in aqueous solution. In the last few years, structural analyses of CT have been carried out by the combined use of two-dimensional (2D) NMR and distance geometry algorithms. These studies indicated that a monomer CT molecule exhibits a well-defined α -helical conformation in the mixed solvents, but not in aqueous solution. For example, NMR studies of salmon CT (sCT) in TFE/H₂O (Meyer et al., 1991), MeOH/H₂O (Meadows et al., 1991), and SDS micelle (Motta et al., 1991a) showed that sCT forms an amphiphilic α -helical structure in the central region. For hCT, it has also been reported to adopt an α -helical structure in TFE/H₂O (Doi et al., 1990). It should be noted, however, that a short double-stranded antiparallel β -sheet structure was obtained in DMSO/H₂O (Motta et al., 1991b). Arvinte et al. (1993) assumed that the α -helix observed by CD in the process of the fibrillation coincides with the amphiphilic α -helix part elucidated by the NMR structural analyses.

The structural information of the fibrillation obtained by CD, fluorescence, and FTIR corresponds to that in the matured stage of the fibrillation. In the present study, the initial stage of the fibrillation before the gelation could be investigated at atomic level by NMR spectroscopy. Recently, the mechanism of the peptide aggregation was extensively studied by NMR spectroscopy for various peptides (Zagorski & Barrow, 1992; Jarvis et al., 1994). However, few attempts have been made to observe the time course of peptide peaks on aggregation or fibrillation on account of the rapid broadening and disappearance of the peptide peaks. To our knowledge, this is the first attempt to measure the time course of the aggregation process by 2D NMR methods.

The present study indicates that the molecular association of hCT is initiated by the intermolecular hydrophobic interaction in the N-terminal and central regions and that the C-terminal region is subsequently involved in the fibrillation.

* Abstract published in *Advance ACS Abstracts*, September 1, 1995.

¹ Abbreviations: CT, calcitonin; hCT, human calcitonin; CD, circular dichroism; FTIR, Fourier transform infrared spectroscopy; sCT, salmon calcitonin; TFE, 2,2,2-trifluoroethanol; MeOH, methanol; SDS, sodium dodecyl sulfate; DMSO, dimethyl sulfoxide; t_f , fibrillation time; 1D, one-dimensional; 2D, two-dimensional; DQFCOSY, double-quantum filtered correlated spectroscopy; HOHAHA, homonuclear Hartmann–Hahn spectroscopy; NOESY, nuclear Overhauser enhancement spectroscopy; TPPI, time-proportional phase incrementation method; ROESY, rotating frame nuclear Overhauser enhancement spectroscopy; NOE, nuclear Overhauser enhancement; H–D, hydrogen–deuterium.

EXPERIMENTAL PROCEDURES

Materials. Synthetic hCT was provided by Ciba-Geigy Pharmaceuticals, Basel, Switzerland.

Sample Preparation. The concentration of hCT was determined from its weight concentration. For resonance assignment, the peptide was dissolved in 90% H₂O/10% D₂O (v/v) solution containing 0.015 M CD₃COOD (pH 2.9). The final concentration of peptide was 20 mg/mL (5.9 mM). It was confirmed that one-dimensional (1D) spectra did not change before and after 2D measurements at this concentration.

For time course experiments, unless otherwise stated, the peptide was dissolved in 100% D₂O solution containing CD₃COOD (pH 2.9), and a series of spectra was recorded; the first spectrum was acquired about 6 min after dissolving the sample in D₂O. Since the fibrillation in the acidic condition proceeds more slowly as compared to the neutral condition, it was decided to use the former condition for this study.

It was confirmed that the fibrillation of hCT in the acidic condition exhibits the same linearity of the logarithm of fibrillation time (t_f) and the logarithm of hCT concentration as that in the neutral condition (Arvinte et al., 1993). The value of t_f is the time corresponding to the intersection with the time axis of the linear increase in turbidity (Arvinte et al., 1993).

NMR Measurements. All proton NMR spectra were recorded on a Bruker AMX600 spectrometer at 300 K. For resonance assignments, DQF-COSY (Piantini et al., 1982; Rance et al., 1983), HOHAHA (Braunschweiler & Ernst, 1983; Davis & Bax, 1985), and NOESY (Jeener et al., 1979; Macura et al., 1981) were run according to the time-proportional phase incrementation method (TPPI) (Marion & Wüthrich, 1983). NOESY spectra were recorded with mixing time of 300 ms, and HOHAHA experiments were acquired with mixing times of 40 and 80 ms. FELIX (Biosym Inc.) was used for data processing and signal assignment on a Silicon Graphics workstation.

For rapid 2D measurements, HOHAHA (mixing time 40 and 80 ms) and ROESY (Bax & Davis, 1985) (mixing time 100 and 200 ms) data were collected by the states-TPPI method (Marion et al., 1989) without phase cycling. Applying this method, it took about 5 min to measure the 256- $(t_1) \times 512$ -(t_2) data matrix. Shifted sine bell squared weight functions were applied in both dimensions, and the data were zero filled to a final size of 1K \times 1K.

RESULTS

Sequential Signal Assignment of hCT. The signal assignment of the hCT spectrum was completed according to the well-established sequential approach (Billeter et al., 1982; Wüthrich et al., 1982). Since this process has been described in great detail in the literature, the details of the assignment process were omitted in this paper. The assignments of the resonances are summarized in Table 1 of the supplementary information. The NH- α fingerprint region of the HOHAHA spectrum at 300 K with 40 ms mixing time showed all expected cross peaks except for Cys¹, Pro²³, and Pro³² (Figure 1). Some additional peaks were observed in the same region, which can be explained by the presence of *cis-trans* isomers of the prolyl residues. The existence of the isomers of the prolyl residues was reported in DMSO and DMSO/H₂O

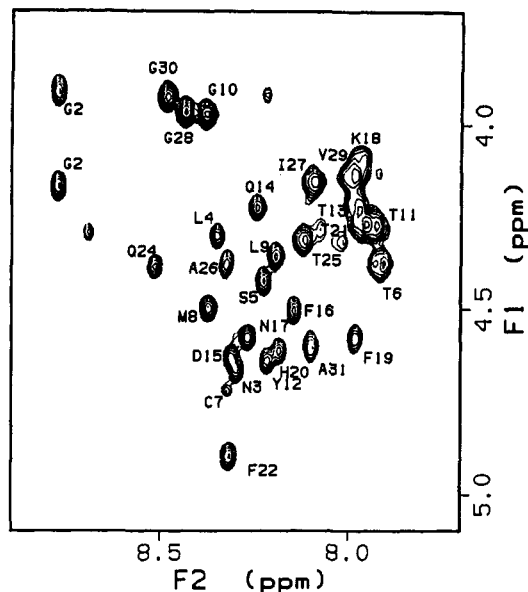


FIGURE 1: Backbone fingerprint region of the HOHAHA (40 ms) spectrum of hCT in 90% H₂O/10% D₂O (pH 2.9) at 300 K. Cross peaks are labeled with their amino acid residue name (single letter code) and sequence numbers.

solution (Motta et al., 1991b) as well as in aqueous solution recently (Kern et al., 1993).

Concentration and Time Dependence of NMR Spectra of hCT in Aqueous Solution. 1D ¹H-NMR spectra of hCT were measured at various concentrations (1, 5, 10, 20, and 80 mg/mL) in 100% D₂O solutions. All spectra were obtained about 6 min after dissolution. There were few differences observed in the chemical shift values and the line widths of nonlabile protons in all the recorded spectra. Some peaks at the concentration of 80 mg/mL shifted slightly (<0.02 ppm), as compared with those at lower concentrations (1–20 mg/mL). Peak intensities increased linearly with an increase of the concentration, as was expected. These results indicate that, just after dissolution (6 min), most of hCT molecules exist as a monomer even at high concentration (80 mg/mL) in aqueous solution.

After 6 min, the spectra of hCT at lower concentrations (1–20 mg/mL) showed little broadening of the line widths without chemical shift change, and no spectral change was observed over 24 h (data not shown). At these low concentrations, the fibrillation would proceed very slowly; therefore, we refer to this condition (20 mg/mL) as the monomer condition.

On the other hand, after 6 min, 1D ¹H-NMR signals of hCT at 80 mg/mL started to show a gradual broadening, but were not accompanied either by any change of chemical shift or by the appearance of new peaks. Around 60 min, a drastic change in the spectra occurred, whereby most of the peptide peaks disappeared (Figure 2). Figure 3 shows the relative intensities of the peptide peaks as a function of time. The change in the NMR spectra at 60 min may be attributed to a transient phase change from particles to a hard, turbid gel. The value of t_f in the acidic condition was estimated to be 40 min by the NMR results, which is equal to the value obtained by absorption measurement (Arvinte et al., 1993). Hereafter, we refer to this condition (80 mg/mL) as the fibril condition.

The water resonance shifted to the downfield and broadened after the change in the peptide peaks at 60 min. This

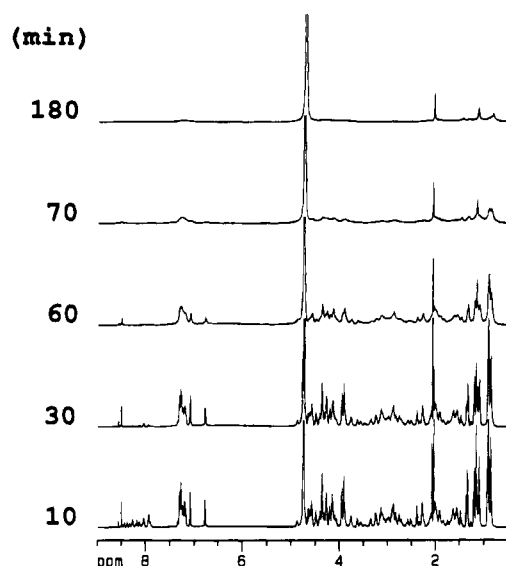


FIGURE 2: Time-course of the ^1H NMR spectra of hCT in the fibril condition (80 mg/mL, pH 2.9, 300 K).

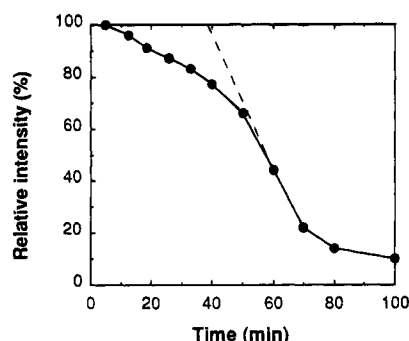


FIGURE 3: Change in time of the averaged intensity of hCT peaks in the 1D ^1H -NMR spectra in the fibril condition. The averaged relative peak heights of resolved nonexchangeable protons are plotted.

phenomenon suggests the formation of a hydrogen bond network among water molecules leading to the gelation of the solution, and subsequent increase in the viscosity.

It should be noted that some peaks in the 1D spectrum remained even at 70 min, whereas the others disappeared completely. This means that all the peaks did not broaden and disappear simultaneously in the course of the fibrillation.

Time-Course of 2D NMR Spectra of hCT in the Fibril Condition. Details of the signal broadening in the fibril condition in D_2O were further investigated for each residue by 2D NMR spectroscopy. The 2D HOHAHA spectrum in the fibril condition which was acquired for 7–13 min after dissolution was almost identical to the spectrum used for the resonance assignment. During the following 30 min, cross peaks broadened gradually, and their intensities became smaller, in accordance with 1D spectra. Figure 4 shows the aliphatic region of the 2D HOHAHA spectrum obtained during the 70–76 min period, when the significant change occurred in the time course of the 1D spectra. Almost all remaining cross peaks in the spectrum corresponded to residues located in the C-terminal region, whereas all peaks of residues in the N-terminal and central regions disappeared. In contrast, some side-chain cross peaks (δ - ϵ of Tyr¹², δ - ϵ of Lys¹⁸, and β - γ of Thr²¹) in those regions did not disappear.

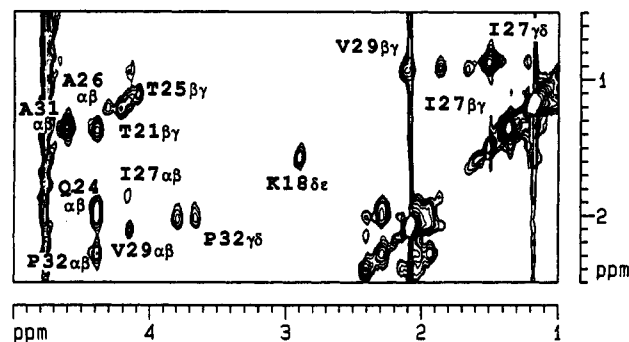


FIGURE 4: Time-course of the aliphatic region of the HOHAHA (40 ms) spectra of hCT in the fibril condition after dissolution for 71–75 min. Cross peaks are labeled with their amino acid residue name (single letter code) and sequence numbers.

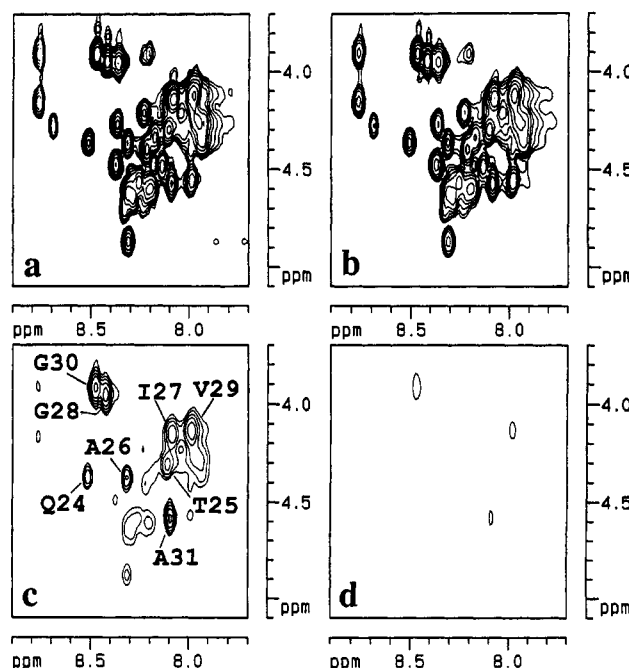


FIGURE 5: Time-course of the fingerprint region of the HOHAHA (40 ms) spectra of hCT in the fibril condition after dissolving hCT in 90% H_2O /10% D_2O , for 7–13 min (a), 30–36 min (b), 44–50 min (c), and 52–58 min (d). Cross peaks are labeled with their amino acid residue name (single letter code) and sequence numbers.

The time course of 1D and 2D HOHAHA spectra in 90% H_2O /10% D_2O in the fibril condition was also conducted in order to examine changes of NH- α cross peaks in the fibril condition. The chemical shifts of some NH- α cross peaks in the fibril condition were slightly different from those in the monomer condition (Figure 5a). All the cross peaks broadened a little with time (Figure 5b), and then, the cross peaks of residues in the N-terminal and central regions broadened and disappeared 40 min after dissolution, but those in the C-terminal region remained (Figure 5c). This broadening feature of the NH- α peaks was identical to that of the cross peaks of aliphatic protons; however, the NH- α peaks disappeared faster than the aliphatic cross peaks (Figure 5d).

ROESY spectra instead of NOESY spectra were measured to obtain spatial information about the fibrillation mechanism since NOESY experiments without phase cycling gave rise to artifacts. The time course of ROESY spectra collection was every 6 min after dissolution, and example spectra (7–13 and 41–47 min after dissolution) are shown in panels a

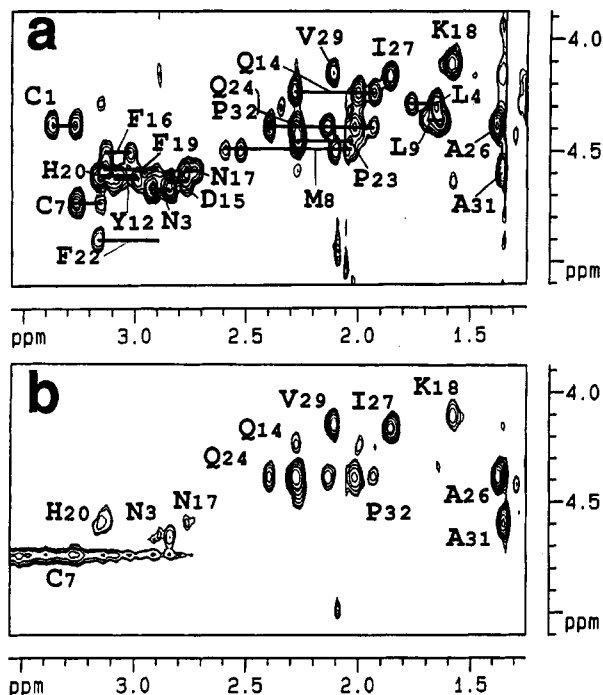


FIGURE 6: The aliphatic region of the ROESY (200 ms) spectra of hCT in the fibril condition after dissolution for 7–13 min (a) and 41–47 min (b).

and b, respectively, of Figure 6. ROESY spectra (mixing time 100 and 200 ms) which were recorded during the fibril formation provided intraresidue and sequential NOEs. Neither long range NOEs nor chemical exchange peaks were observed for both mixing times. The α - β intraresidue NOE cross peaks of the C-terminal region (Ala^{26,31}, Ile²⁷, Val²⁹, and Pro³²) are scarcely changed between panels a and b of Figure 6. As for the N-terminal and central residues, the cross peaks of Cys¹, Leu^{4,9}, Met⁸, Tyr¹², Asp¹⁵, and Phe^{16,19,22} (group A) disappeared, but the peaks of Asn^{3,17}, Cys⁷, Gln¹⁴, Lys¹⁸, and His²⁰ (group B) remained weak. The α - β cross peak of Ser⁵ also remained weak in the same ROESY spectrum (data not shown), but the signal change of threonine residues was not clearly observed because of overlapped artifacts near diagonal peaks. These were the cases for both ROESY spectra of mixing time 100 and 200 ms.

Hydrogen–Deuterium (H–D) Exchange Experiments. Generally speaking, H–D exchange experiments of amide protons offer information about hydrogen bonding derived from secondary structure and solvent accessibility to the peptide backbone. Figure 7 displays the 1D spectra of NH proton regions for the fibril (a) and monomer (b) conditions, respectively. The spectra of the monomer condition remained unchanged, except for the labile NH protons, for the first 3 h. The two sharp, unaltered peaks at 8.51 and 8.57 ppm are the C₂ protons of His²⁰ in the *trans* and *cis* isomers, respectively (Kern et al., 1993).

The 1D spectra at 6, 12, and 24 min in the fibril and monomer conditions show that NH peaks in the fibril condition disappeared slower than those in the monomer condition, despite broadening of the peaks by the fibrillation in the fibril condition. The anomalous behavior in the signal disappearance between the fibril and monomer conditions can be attributed to differences in their respective H–D exchange rates. Namely, the H–D exchange would proceed more slowly in the fibril condition compared to the monomer

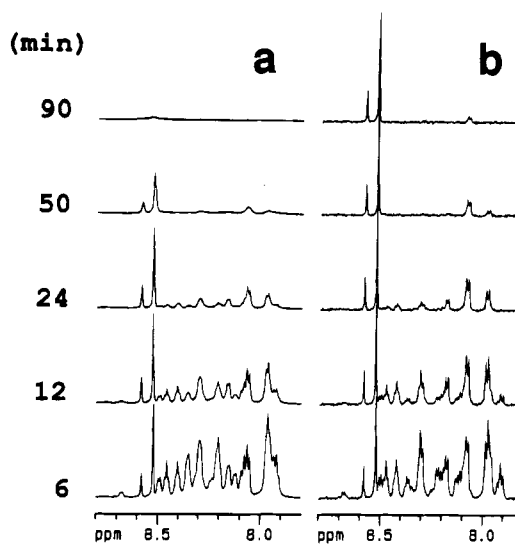


FIGURE 7: Time-course of the NH signals of hCT in the fibril condition (a) and in the monomer condition (b).

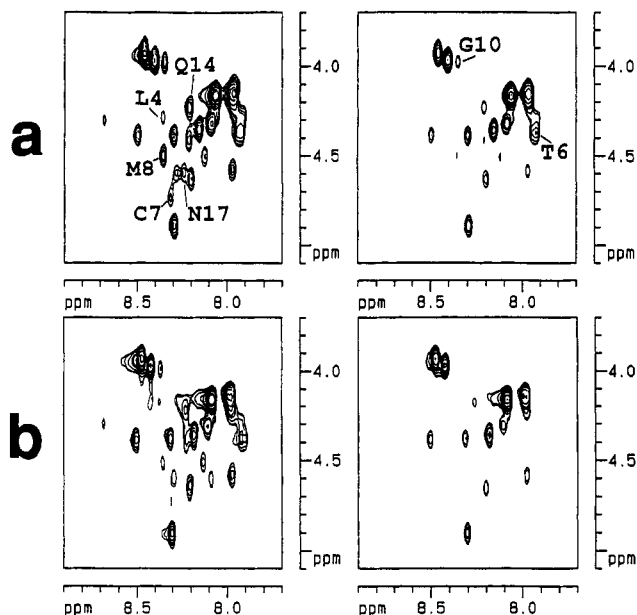


FIGURE 8: Time-course of the fingerprint region of the HOHAHA (40 ms) spectra of hCT in the fibril (a) and monomer (b) condition for 7–13 min (left), and 13–19 min (right) after dissolution. Labels with their amino acid residue name (single letter code) and sequence number indicate cross peaks whose H–D exchange rates in the fibril condition are slower than those in the monomer condition.

condition. Almost all the NH protons exchanged with D₂O for a period of 50 min after dissolution.

In order to study specific details of the H–D exchange of the NH protons, the time course of 2D HOHAHA spectra was measured for both conditions after dissolution. Some cross peaks (Leu⁴, Thr⁶, Cys⁷, Met⁸, Gly¹⁰, Gln¹⁴, and Asn¹⁷) disappeared significantly more slowly in the fibril condition (upper in Figure 8) than those in the monomer condition (lower in Figure 8). All these residues are located in the N-terminal and central regions. Thus, the H–D exchange rates of these residues in the fibril condition would be slower than those in the monomer condition. There was no discernible difference in the H–D exchange rates of the C-terminal residues between the fibril and monomer condition.

DISCUSSION

The hCT fibrillation mechanism conforms to the double nucleation mechanism (Arvinte et al., 1993), which postulates that polymers form by nucleation processes and that there are two clear pathways for nucleation. The first nucleation process takes place in the bulk solution and is called homogeneous nucleation. The second nucleation occurs on the surface of pre-existing polymers. This second process is called heterogeneous nucleation. Aggregate formation in either case is thermodynamically unfavorable until a critical nucleus size is reached (Ferrone et al., 1980, 1985; Samuel et al., 1990).

The gradual signal broadening in the spectra for 40 min after the dissolution would arise from the thermodynamically unfavorable association of monomer molecules before the formation of the critical nucleus, and the second rapid broadening would be attributed to the further development of the critical nucleus in the homogeneous nucleation. All the spectral changes observed by NMR occur around t_f and could not provide us with information in the further maturing processes observed by electron microscopy, such as growth and thickening of fibrils and development of new fibrils from the existing one in the heterogeneous nucleation.

The gradual broadening may be caused by slow interconversions between a mixture of conformations within the NMR time scale, as reported in β -amyloid peptides (Zagorski & Barrow, 1992). The slight difference in the chemical shifts between the fibril and monomer condition might be one proof of the interconversions between monomer and associated hCT molecules. The observed chemical shifts of the peptide peaks would reflect averaged structure of the monomer and associated hCT. The chemical shift and/or J coupling in the associated hCT would differ from those in the monomer hCT, which causes the exchange broadening.

Thermodynamic study indicated that protein association consists of two steps, that is, the mutual penetration of hydration layers, causing disordering of the solvent, followed by further short range interactions (Ross & Subramanian, 1981). During the hCT fibrillation, the cross peaks of C α and exchangeable NH proton broadened and disappeared faster than those among nonexchangeable protons. The hydration layer of the associated hCT would be expected to differ from that of the monomer. The change in hydration layer of the associated hCT will be one of the reasons for the signal broadening.

Consequently, residues whose peaks broaden faster are strongly involved in the association before the gelation. However, after the gelation, the increase in viscosity is a dominant factor for the rapid broadening.

In TFE/H₂O solution, hCT consists of an α -helix in the central region (Doi et al., 1990). The α -helix is reported to be of the amphiphilic type, where all hydrophobic residues are oriented toward one side (Figure 9). The hydrophobic side of the helix contains Met⁸, Leu⁹, Tyr¹², Asp¹⁵, and Phe^{16,19,22}. All these residues belong to group A, whose ROESY cross peaks disappeared faster in the course of the fibrillation. On the other hand, the hydrophilic side contains residues belonging to group B, whose ROESY peaks disappeared slowly (Figure 8). These results suggest that the residues of group A participate in the initial association step and that the hydrophobic intermolecular interaction between residues of group A is particularly important for

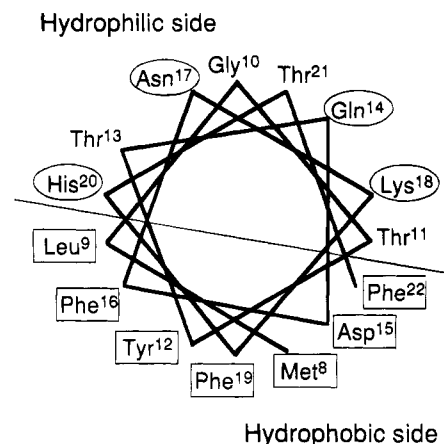


FIGURE 9: Helical wheel model of hCT in the residue range (Met⁸–Phe²²). Square boxes indicate the residues whose peak belong to group A, whereas circle boxes indicate those belonging to group B.

the association of hCT. If hCT molecules are associated by the hydrophobic interaction of the residues in the group A, the initial cluster might be a helical bundle where the hydrophobic sides of the amphiphilic helices interact with each other. This idea is in accord with the CD results of hCT fibrillation that suggest hCT takes an α -helical structure with time (Arvinte et al., 1993). Recent study on the self-association of N-terminal fragments of barnase suggested that such an amphiphilic feature of peptide could contribute to the formation of a stable helical structure through aggregation (Yoshida et al., 1993).

The ROESY cross peaks of the N-terminal residues, Cys¹ and Leu⁴, also disappeared rapidly, despite the fact that they are not included in the amphiphilic helix part. An explanation for this behavior is that Leu⁴ is located at the starting point of the α -helix (Motta et al., 1991a) and that the β -protons of Cys¹, which are located near Met⁸ and Leu⁹, become involved in the hydrophobic cluster.

The previous results obtained by FTIR (Arvinte et al., 1993) suggested the existence of an intermolecular β -sheet in the tail region (residues 23–32) of the matured hCT fibrils 1000 min after dissolution. The broadening feature of the peaks in the C-terminal region suggests that it takes part in the fibrillation after the interaction of the N-terminal and central regions (e.g., helical bundle formation). The C-terminal region may orient the helical bundles by forming intermolecular β -sheet, leading to development of the aggregates.

As mentioned above, there is chemical exchange between the monomer and associated hCT. The slow H–D exchange rate of the N-terminal and central residues in the fibril condition indicates hydrogen bond formation in these regions of the associated hCT. The intermolecular side-chain to backbone amide hydrogen bonding would occur during the aggregation, as reported for amyloid β -peptides (Zagorski & Barrow, 1992). It would also be possible that the formation of intramolecular hydrogen bonds is induced by secondary structure stabilized by intermolecular interactions, such as hydrophobic interaction.

The fibrillation of sCT occurs much slower than that of hCT, and sCT is highly stable in aqueous solution (Arvinte et al., 1993). The comparison of amino acid sequence of hCT and sCT shows only small differences in the respective

hydrophobicity for each residue in the hydrophobic side of the amphiphilic helix of hCT(→sCT); Met⁸(→Val), Tyr¹²(→Leu), Asp¹⁵(→Glu), Phe¹⁶(→Leu), Phe¹⁹(→Leu), and Phe²²(→Tyr). This suggests that the difference in the fibrillation features between hCT and sCT arises from the overall electrostatic and hydrophobic effects of the molecule.

The dissolution of lyophilized powder of hCT fibrils in aqueous solution caused rapid development of fibrils. Furthermore, it was also found that urea acts as a reagent to prevent fibril development of hCT. This effect is now under investigation in our laboratory.

We interpret the hCT fibrillation process in terms of the following model: In the homogeneous nucleation step, the association of hCT monomers proceeds by the intermolecular hydrophobic interaction of the residues in the N-terminal and central regions. The amphiphilicity of hCT is important for the hydrophobic interaction, and the helical bundle might be formed in the critical nucleus, which in turn induces the formation of the hydrogen bonds. The C-terminal region subsequently becomes a template for the α -helical rods in the following stage of the fibrillation (Arvinte et al., 1993).

ACKNOWLEDGMENT

We thank Drs. R. Andreatta, B. Kamber, and B. Riniker for providing the sample of hCT and supporting this work. We also thank Drs. M. J. J. Blommers and T. Arvinte for helpful discussions. We are grateful to K. Gohda for critically reading the manuscript and encouragement for this work.

SUPPORTING INFORMATION AVAILABLE

One table showing chemical shift data of hCT (20 mg/mL) in aqueous solution, pH 2.9, 300 K (1 page). Ordering information is given on any current masthead page.

REFERENCES

- Arvinte, T., & Ryman, K. (1992) European Patent Application, Publication Number 0490549A.
- Arvinte, T., Cudd, A., & Drake, A. F. (1993) *J. Biol. Chem.* **268**, 6415–6422.
- Austin, L. A., & Heath, H. (1981) *N. Engl. J. Med.* **304**, 296–297.
- Bax, A., & Davis, D. G. (1985) *J. Magn. Reson.* **63**, 207–213.
- Billeter, M., Braun, W., & Wüthrich, K. (1982) *J. Mol. Biol.* **155**, 321–346.
- Braunschweiler, L., & Ernst, R. R. (1983) *J. Magn. Reson.* **53**, 521–528.
- Copp, D. H., Cameron, E. C., Cheney, B. A., Davidson, A. G. F., & Henze, K. G. (1962) *Endocrinology* **70**, 638–649.
- Davis, D. G., & Bax, A. (1985) *J. Am. Chem. Soc.* **107**, 2820–2821.
- Doi, M., Yamanaka, Y., Kobayashi, Y., Kyogoku, Y., Takimoto, M., & Goda, K. (1990) *Peptides: Chemistry, Structure & Biology*, 11th Proc. Am. Pept. Symp., July 9–14, 1989, La Jolla, CA (Rivier, J. E., & Marshall, G. R., Eds.) pp 165–167, ESCOM, Leiden, The Netherlands.
- Ferrone, F. A., Hofrichter, J., Sunshine, H. R., & Eaton, W. A. (1980) *Biophys. J.* **32**, 361–380.
- Ferrone, F. A., Hofrichter, J., & Eaton, W. A. (1985) *J. Mol. Biol.* **183**, 611–631.
- Jarvis, J. A., Munro, S. L. A., & Craik, D. J. (1994) *Biochemistry* **33**, 33–41.
- Jeener, J., Meier, B. H., Bachmann, P., & Ernst, R. R. (1979) *J. Chem. Phys.* **71**, 4546–4553.
- Kern, D., Drakenberg, T., Wikström, M., Forsén, S., Bang, H., & Fischer, G. (1993) *FEBS Lett.* **323**, 198–202.
- Kumar, M. A., Foster, G. V., & MacIntyre, I. (1963) *Lancet* **2**, 480–482.
- Macura, S., Huang, Y., Suter, D., & Ernst, R. R. (1981) *J. Magn. Reson.* **43**, 259–281.
- Marion, D., & Wüthrich, K. (1983) *Biochem. Biophys. Res. Commun.* **113**, 967–974.
- Marion, D., Ikura, M., Tschudin, R., & Bax, A. (1989) *J. Magn. Reson.* **85**, 393–399.
- Meadows, R. P., Nikonowicz, E. P., Jones, C. R., Bastian, J. W., & Gorenstein, D. G. (1991) *Biochemistry* **30**, 1247–1254.
- Meyer, J. P., Pelton, J. T., Hoflack, J., & Saudek, V. (1991) *Biopolymers* **31**, 233–241.
- Motta, A., Pastore, A., Goud, N. A., & Morelli, M. A. C. (1991a) *Biochemistry* **30**, 10444–10450.
- Motta, A., Temussi, P. A., Wünsch, E., & Bovermann, G. (1991b) *Biochemistry* **30**, 2364–2371.
- Piantini, U., Sørensen, O. W., & Ernst, R. R. (1982) *J. Am. Chem. Soc.* **104**, 6800–6801.
- Rance, M., Sørensen, O. W., Bodenhausen, G., Wagner, G., Ernst, R. R., & Wüthrich, K. (1983) *Biochem. Biophys. Res. Commun.* **117**, 479–485.
- Ross, P. D., & Subramanian, S. (1981) *Biochemistry* **20**, 3096–3102.
- Samuel, R. E., Salmon, E. D., & Briehl, R. W. (1990) *Nature* **345**, 833–835.
- Sieber, P., Riniker, B., Brugger, M., Kamber, B., & Rittel, W. (1970) *Helv. Chim. Acta* **53**, 2135–2150.
- Wüthrich, K., Wider, G., Wagner, G., & Braun, W. (1982) *J. Mol. Biol.* **155**, 311–319.
- Yoshida, K., Shibata, T., Masai, J., Sato, K., Noguti, T., Go, M., & Yanagawa, H. (1993) *Biochemistry* **32**, 2162–2166.
- Zagorski, M. G., & Barrow, C. J. (1992) *Biochemistry* **31**, 5621–5631.

BI951156S